Original Article | Basic and Mechanism Sciences

Amniotic fluid stem cell conditioned medium's role in Schwann cell proliferation, survival, and cellular antioxidant activity under normative and oxidative stress conditions

Chukwuweike Gwam^, Nequesha Mohamed, Ayobami S. Ogunsola, Marcel G. Brown, Kaitlin A. Henry, Xue Ma

Department of Orthopaedic Surgery and Rehabilitation, Atrium Wake Forest Baptist Health, Winston-Salem, NC, USA

Contributions: (I) Conception and design: C Gwam, X Ma, N Mohamed; (II) Administrative support: AS Ogunsola, MG Brown, KA Henry, X Ma; (III) Provision of study materials or patients: C Gwam, X Ma; (IV) Collection and assembly of data: C Gwam, X Ma, N Mohamed; (V) Data analysis and interpretation: C Gwam, X Ma, MG Brown, AS Ogunsola; (VI) Manuscript writing: All authors; (VII) Final approval of manuscript: All authors.

Correspondence to: Chukwuweike Gwam, MD, MBA. Department of Orthopaedic Surgery and Rehabilitation, Atrium Wake Forest Baptist Health, One Medical Center Boulevard, Winston-Salem, NC 27157, USA. Email: cgwam1988@gmail.com.

Background: Peripheral nerve injuries present a major clinical challenge due to their high morbidity and often incomplete recovery of function. While autografts remain the gold standard for nerve repair, their use is constrained by limited donor availability and donor site complications. Alternative strategies, such as allografts and tissue-engineered grafts, have been developed but are still associated with suboptimal outcomes, including chronic pain and sensory disturbances. Thus, there is a need for novel therapies that can enhance nerve regeneration. Amniotic fluid stem cell conditioned medium (AFS-CM) houses regenerative properties that may be useful in peripheral nerve injury. This study aims to assess the role of AFS-CM on Schwann cell survival and proliferation under normative and oxidative stress conditions, preventing oxidative stress-induced premature senescence of Schwann cells *in vitro* and maintaining cellular redox homeostasis.

Methods: Primary Schwann cells were treated with various concentrations of AFS-CM. Cell proliferation was assessed using the Cell Counting Kit-8 (CCK-8) assay, and viability under oxidative stress was measured after exposing cells to hydrogen peroxide (H_2O_2). Reactive oxygen species (ROS) levels and both catalase and superoxide dismutase (SOD) levels were evaluated. Cellular senescence markers were also assessed to determine AFS-CM's protective effects.

Results: AFS-CM treatment resulted in a dose-dependent increase in Schwann cell proliferation ($P<0.05$). Under oxidative stress conditions, AFS-CM significantly improved cell viability compared to controls ($P<0.05$). ROS levels were markedly reduced in AFS-CM-treated cells ($P<0.05$), and this was accompanied by upregulation of catalase and SOD expression ($P<0.05$). Moreover, AFS-CM reduced stress-induced cellular senescence, as indicated by decreased senescence-associated β-galactosidase activity and lower expression of senescence markers ($P<0.05$).

Conclusions: AFS-CM enhances Schwann cell proliferation, viability, and resistance to oxidative stress, while reducing cellular senescence. These findings suggest that AFS-CM could be a promising adjunctive therapy for peripheral nerve injuries by promoting Schwann cell resilience and regenerative capacity. Future studies are needed to validate these *in vitro* results *in vivo* and explore their potential clinical application for improving functional recovery in patients with peripheral nerve damage.

Keywords: Amniotic fluid stem cells; peripheral nerve injury; Schwann cells; oxidative stress

Submitted May 29, 2024. Accepted for publication Feb 10, 2025. Published online Feb 25, 2025.
doi: 10.21037/atm-24-107
View this article at: https://dx.doi.org/10.21037/atm-24-107

^ ORCID: 0000-0003-0579-3524.

Introduction

Peripheral nerve injuries present a significant clinical challenge for care providers and often result in significant morbidity and incomplete recovery of function despite timely intervention (1-3). Autograft repair remains the gold-standard treatment modality for peripheral nerve injuries unable to be addressed with direct end-to-end repair. Unfortunately, its use is often limited by factors like donor site morbidity and restricted graft availability (4,5). While alternative methods, such as allografts and tissue-engineered nerve grafts, exist, they fail to achieve optimal functional recovery for many patients, with up to 50% experiencing ongoing dysfunction, pain, or dysesthesias (6).

Peripheral nerve recovery following injury is a complex physiological process initiated by Wallerian degeneration, which involves the breakdown of the axon and myelin sheath distal to the injury site (7-10). This is followed by the recruitment of inflammatory cells, such as macrophages and neutrophils, which clear debris and release factors that support nerve repair. Schwann cells are crucial in this regenerative process. They dedifferentiate and proliferate to form the Bands of Büngner, a structure that guides the regrowth of axons. Additionally, Schwann cells secrete neurotrophic factors and modify the extracellular matrix, thus providing both structural and biochemical support for nerve regeneration (11-13).

The ability of Schwann cells to survive and proliferate in the inflammatory microenvironment post-injury is critical, as exposure to higher levels of oxidative stress can impair Schwann cell function (14). Previous studies have revealed that Schwann cell senescence, secondary to oxidative stress, can be a culprit for incomplete recovery after peripheral nerve injury (15-17). As such, enhancing Schwann cell resilience is essential for successful nerve regeneration. Emerging therapeutic strategies utilizing cell-based approaches have been developed to enhance Schwann cell function and modulate the inflammatory response, potentially improving the efficacy of nerve repair techniques.

Schwann cell transplantation techniques aim to facilitate peripheral nerve regeneration after injury (18). These techniques involve harvesting Schwann cells from healthy peripheral nerves, subsequent *in-vitro* expansion, and then reimplanting donor Schwann cells to peripheral nerve injury sites in adjunct with a nerve scaffold. While this may offer some clinical benefits, its use is limited by the costs and lead time required to acquire, expand, and reimplant native Schwann cells to the injury site. Nonetheless, cell-based therapies offer promise in facilitating peripheral nerve recovery. The regenerative nature of stem cell transplantation and other cell-based therapies have been attributed to the paracrine effects of transplanted stem cells on local tissue environments, specifically in creating a favorable redox environment conducive to tissue regeneration (19,20). As such, increasing interest has been in using highly concentrated stem cell conditioned medium in regenerative medicine (19). Human amniotic fluid-derived stem cells can be conveniently collected after childbirth and harvested for therapeutic use. Additionally, amniotic fluid stem cell conditioned medium (AFS-CM) may serve as a valuable option due to the high passage capacity of amniotic fluid stem cells. Furthermore, the lack of immunogenic and tumorigenic potential and the practical applicability of AFS-CM pose it as a promising adjunct treatment for peripheral nerve injury (19).

The present study assesses the effects of AFS-CM on Schwann cell viability and proliferation. More specifically,

Highlight box

Key findings

- Amniotic fluid stem cell conditioned medium (AFS-CM) significantly enhances Schwann cell proliferation and viability, particularly under oxidative stress conditions.
- AFS-CM reduces cellular reactive oxygen species levels by upregulating key antioxidant enzymes, such as catalase and superoxide dismutase.
- AFS-CM mitigates stress-induced senescence in Schwann cells, thereby promoting cellular resilience.

What is known and what is new?

- Current therapies for peripheral nerve injuries, including autografts and allografts, often yield incomplete functional recovery, with limited efficacy in promoting nerve regeneration and Schwann cell resilience under stress conditions.
- This study introduces AFS-CM as a novel therapeutic agent that enhances Schwann cell function, providing protective effects against oxidative stress and cellular senescence, which could potentially improve outcomes in nerve repair.

What is the implication, and what should change now?

- The findings suggest that AFS-CM may serve as a viable adjunct therapy for peripheral nerve injuries, enhancing Schwann cell-mediated nerve regeneration and reducing long-term complications.
- Further *in vivo* studies should be conducted to validate these findings and explore the therapeutic potential of AFS-CM in clinical settings, potentially leading to new treatment protocols for peripheral nerve repair.

we explore the role of AFS-CM on Schwann cell survival and proliferation under normative and oxidative stress conditions, preventing oxidative stress-induced premature senescence of Schwann cells *in vitro* and maintaining cellular redox homeostasis. We present this article in accordance with the ARRIVE reporting checklist (available at https://atm.amegroups.com/article/view/10.21037/atm-24-107/rc).

Methods

Isolation and culture of primary rat Schwann cells

The experiments of the present study were approved by the Institution of Animal Care and Use Committee (IACUC) at Atrium Wake Forest Baptist Health (IACUC # A19-101), in compliance with institutional guidelines for the care and use of animals. A protocol was prepared for this study without registration. Schwann cells were obtained and isolated from adult male Lewis rats obtained from Charles Rivers Laboratories using a protocol previously described by Haastert *et al.* (21). Briefly, the sciatic nerve from male Lewis rats was harvested in a pre-degenerated state and prepared for Schwann cell isolation. Sciatic nerve epineurium was dissected from the nerve harvest, and the resulting epineural-free nerve was transferred in Dulbecco's Modified Eagle Medium (DMEM) with 1% penicillin/streptomycin (pen/strep; Thermo Fisher Scientific, Waltham, MA, USA, Catalog number 15140122) (22) to a sterile workstation. Nerve tissue was washed in DMEM and cultured onto non-coated wells on a six-well plate with DMEM + 10% fetal bovine serum (FBS; Thermo Fischer Scientific, Catalog number A5256801) (23) + 1% pen/strep. Schwann cells were subsequently dissociated from the tissue by adding 0.125% collagenase + 1.25 U mL^{-1} dispase to create a dissociation medium. The tissue was then incubated with the dissociation medium for 20 hours at 37 ℃ with 5% carbon dioxide (CO_2). The resulting tissue was separated mechanically by gentle trituration until a homogenous solution was obtained, after which samples were centrifuged at 235 g for 5 min at 21 ℃. A pellet was formed after centrifugation and re-suspended in DMEM + 10% FBS + 1% pen/strep and 1% glutamate. The cell pellet was expanded in laminin + poly-L-ornithine (Sigma Aldrich, Milwaukee, WI, USA) coated flasks until ~70–80% confluence. The resultant cell passage was passed and maintained in DMEM + 10% dimethyl sulfoxide (DMSO) solution and stored in liquid nitrogen until further use. All cell stocks were thawed and passed once before being used for *in-vitro* experiments.

Verification of Schwann cell purity

Primary cultured rat Schwann cells were fixed with 4% paraformaldehyde in phosphate buffered saline (PBS, Thermo Fisher Scientific) at 37 ℃ for 15 min. Fixed cells were washed with PBS and permeabilized using PBS containing 0.3% Triton X-100 then blocked with 10% rabbit serum for 30 min at 37 ℃. Cells then were incubated at 4 ℃ overnight with primary S100 antibody (1:500, Abcam, Cambridge, UK) then Alexa Fluor 488-conjugated secondary antibody for 30 min at 37 ℃ (Thermo Fisher, Waltham, MA, USA). Cell nuclei were counterstained with 4',6-diamidino-2-phenylindole (DAPI) (1:5,000, Thermo Fisher). Cells were imaged using a fluorescent microscope (Olympus, Japan). Confirmation of Schwann cell phenotype can be seen in *Figure 1*.

Formulation and characterization of AFS-CM

Amniotic fluid stem cells were obtained from Nutech Inc. (Birmingham, AL, USA) and cultured in DMEM (Corning, NY, USA; Product number 15-018-CV) with 20% FBS in a T175 flask (Thermo Fisher Scientific) until ~80% confluence, after which cells were maintained in serum-free DMEM for 24 hours. Passage two to four cultured amniotic fluid stem cells were used in this study. The conditioned medium was then collected and centrifuged at 4 ℃ at 3,000 g for 5 min. After that, the centrifuged medium was re-centrifuged with ultra-centrifugal filters (Thermo Fisher Scientific) (24) with a semipermeable membrane of 100kDa at 4 ℃, 3,000 g for 2 hours. This was done to purify the AFS-CM formulation.

The resulting supernatant solution was collected and stored at −80 ℃ until further use. According to the manufacturer's instructions, protein content was measured using a Bradford protein assay kit (Thermo Fisher Scientific, Product number A55866) (25). Three separate Bradford protein assay sample measurements were used to quantify the mean protein amount in each AFS-CM batch. The cytokines and growth factors of the AFS-CM were analyzed using a multiplex customized Quantibody human enzyme-linked immunosorbent assay (ELISA) array (Raybiotech, peachtree Corners, GA, USA) that detected 39 different cytokines and growth factors. The cytokines with the top 5 greatest concentrations included, insulin-like growth factor binding protein (IGFBP), bone morphogenetic protein

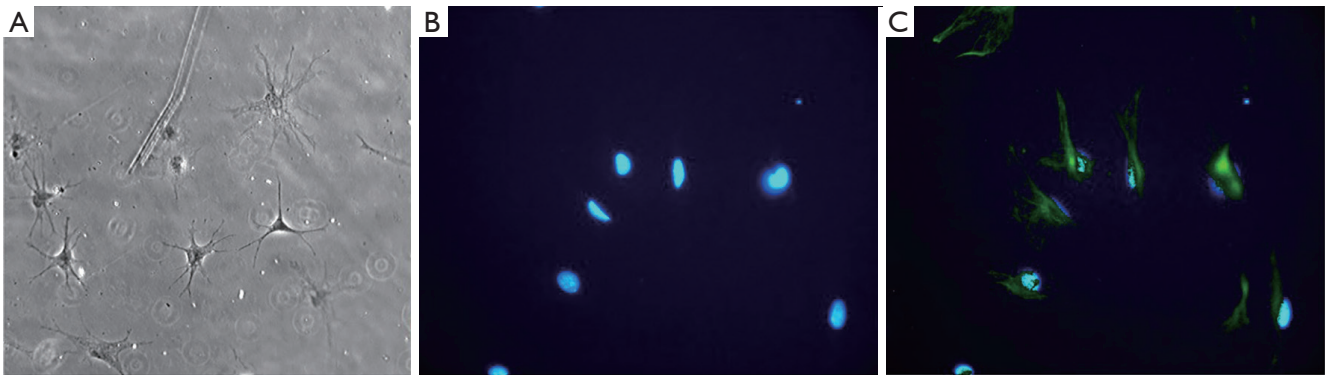

Figure 1 Immunofluorescence analysis of primary cultured rat Schwann cells. (A) A bright-field image displaying primary cultured rat Schwann cells before staining. The image reveals the characteristic spindle-shaped morphology of Schwann cells, with processes extending from the cell bodies (magnification ×200). (B) Fluorescence image showing the nuclei of Schwann cells stained with DAPI (blue). The DAPI staining highlights the nuclear localization within the cells, confirming the presence of Schwann cells in the culture (magnification ×200). (C) Fluorescence image showing Schwann cells stained with an anti-S100 antibody (green), a specific marker for Schwann cells. The green fluorescence indicates successful labeling of the S100 protein within the Schwann cells' cytoplasm. The overlay with DAPI staining (blue) in this panel demonstrates the colocalization of S100 protein within the cells, confirming their identity as Schwann cells (magnification ×200). DAPI, 4',6-diamidino-2-phenylindole.

(BMP), transforming growth factor beta (TGFβ), basic fibroblast growth factor (bFGF) and insulin-like growth factor (IGF) (level of detection: 793.8±69.6, 313.3±52.1, 188.3±33.6, 145.7±30.2, 124.6±31.1 pg/mL, respectively).

Schwann cell proliferation test

96 well plates were used with wells pre-coated with laminin + poly-L-ornithine (Sigma Aldrich, Milwaukee, WI, USA). The well-coating procedure was previously described by Ma *et al.* (26). Primary rat Schwann cells (passages 3 to 5) were plated (4×10^3) on a 96 well plate in DMEM (Corning, Product number 15-018-CV) + 10% FBS medium + 1% glutamax (Thermo Fisher Scientific, Catalog number: A1286001) (25) + 0.1% forskolin (100 µL) until 50–60% confluence. Medium was then exchanged with DMEM + 1% FBS with varying concentrations of AFS-CM (0, 1, 10, and 20 µg/mL). Cell proliferation was assessed at one day, three days, and five days after using a Cell Counting Kit-8 (CCK-8) assay (Dojindo, Kumamoto, Japan, product number: CK04) (27) according to the manufacturer's instructions. Briefly, 10ul of cell proliferation reagent water-soluble tetrazolium-1 (WST-1) was added to each cell culture well at the previously stated time points and incubated for 1 hour. WST-1 is a stable tetrazolium salt cleaved by nicotinamide adenine dinucleotide phosphate [NAD(P)H] in viable cells. Once reduced, WST-1 emits a formazan dye. The amount of formazan die emitted directly correlates to the number of viable cells. Absorbance was measured at 450 nm after 1 hour using a standard microplate reader.

Schwann cell viability under oxidative stress

A lethal dose curve was generated to ascertain the hydrogen peroxide (H_2O_2) concentration necessary to reduce primary Schwann cell culture (4×10^3) by 50% on a pre-coated 96-well plate (Thermo Fisher Scientific) (28). H_2O_2 concentrations used were 0, 20, 50, 80, 100, 500 µM, and 1 mM. The ascertained dose was 80 µM of H_2O_2. Primary Schwann cells were then plated (4×10^3) on a 96-well pre-coated plate and incubated until 60–70% confluence in DMEM + 10% FBS medium (100 µL). The medium was then exchanged with DMEM + 1% FBS (100 µL) with varying concentrations of AFS-CM (0, 1, 10, and 20 µg/mL) for twelve hours, after which cell culture was exposed to 80 µM of H_2O_2 for 1 hour. Medium was subsequently exchanged to DMEM + 10% FBS medium (100 µL). Cell culture medium was exchanged with DMEM + 1% FBS + varying concentrations of AFS-CM (0, 1, 5, 10, 20 µg/mL) every 24 hours, thereby ensuring the continued delivery of AFS-CM. Cell viability was assessed at 24 and 48 hours using a CCK-8 (Dojindo, product number: CK04) (27) according to the manufacturer's instructions.

Reactive oxygen species (ROS) generation

6-well plates were pre-coated with laminin + poly-L-ornithine then plated with primary Schwann cells (4×10^3; passages 3 to 5) in DMEM + 1% FBS medium (100 µL) + varying concentrations of AFS-CM (0, 1, 10, and 20 µg/mL) until 60–70% confluency. Cells were washed in phosphate-buffered saline (PBS; Thermo Fisher Scientific, Catalog number: 10010023) and treated with 0 µM, 100 µM, 1 mM, or 4 mM H_2O_2 for 15 min in DMEM + 1% FBS medium. Cellular ROS were quantified for the cell culture using the cellular ROS detection kit (Abcam, product number: ab186027) (29) according to the manufacturer's instructions. The fluorescence signal was read by a fluorescence microplate reader (Thermo Fisher Scientific) at Ex/Em =520/605 nm (30). An analysis of variance (ANOVA) was conducted to assess the fold change difference between groups.

Quantifying Schwann cell senescence

Six-well plates were coated with laminin + poly-L-ornithine and then plated with primary Schwann cells (1×10^4; passages 3 to 5) in DMEM + 10% FBS medium + 1% penicillin/streptomycin + 1% glutamine until 60–70% confluency. Cells were then washed in PBS, and the medium was exchanged to DMEM + 10% FBS medium with varying concentrations of AFS-CM (0, 1, 10, and 20 µg/mL). Oxidative stress-induced senescence was initiated using an adapted protocol from Wang *et al.* (31). Briefly, cells were exposed to 20 µM of H_2O_2 for 15 min in DMEM + 1% FBS medium then washed with PBS after H_2O_2 exposure, and medium was exchanged with DMEM + 10% FBS + varying concentrations of AFS-CM (0, 1, 10, and 20 µg/mL) for 24 hours. The process was then repeated with 10 µM of H_2O_2 for another 24 hours to assess the protective effects of AFS-CM on cell survival against oxidative stress. Cells were then stained for S-beta-galactosidase using the senescence b-galactosidase staining kit (Abcam, product number: ab102534) (32) according to the manufacturer's instructions. Positive and negatively stained cells were counted. An ANOVA was performed to compare the percent difference in cells staining positive when compared to the control group (no H_2O_2 and no AFS-CM).

Superoxide dismutase (SOD) and catalase measurement

Primary Schwann cells (passages 3 to 5) were then plated (4×10^3) on a 96-well plate and incubated until 60–70% confluence in DMEM + 10% FBS medium. The medium was then exchanged with DMEM + 1% FBS with varying concentrations of AFS-CM (0, 1, 10, and 20 µg/mL) for 12 hours. The catalase activity assay kit (Abcam, product number: ab83464) (33) was used to measure catalase activity at an optical density (OD) 570 nm colorimetrically according to the manufacturer's instructions. In this assay, a proprietary probe reacts with unconverted H_2O_2 to produce a product that can be measured colorimetrically. Thus, the signal intensity is inversely proportional to catalase activity. SOD activity was calculated using an SOD activity assay kit (Abcam, product number: ab65354) (34) which measures the inhibition of xanthine oxidase by SOD. This assay kit was used according to the manufacturer's instructions. An ANOVA was conducted to assess the fold change difference between groups.

Statistical analysis

Continuous data was analyzed using a one-way ANOVA. An ANOVA *post-hoc* Tukey's honestly significant difference (HSD) was performed to assess multiple comparisons of mean diff differences between groups. Statistical significance was established at a P value threshold of less than 0.05. All statistical tests were two-sided and performed using Python's SciPy and Pandas libraries. Data visualization was facilitated through the Matplotlib and Seaborn libraries.

Results

Protein concentration of AFS-CM

AFS-CM samples (n=28 from four cell lines) were examined utilizing Bradford protein analysis to estimate protein quantities. The mean protein concentration of the AFS-CM samples was 1,918.33 µg/mL, with a standard deviation of 909.74 µg/mL. The protein concentration was highly variable, with our Bradford protein analysis revealing a range in protein content from 305.90 to 4,276.62 µg/mL. To account for this variability, all AFS-CM samples were pooled and used at the indicated concentrations for the experiments, minimizing the potential for technical batch effects from different cultures.

AFS-CM promotes Schwann cell proliferation under normative conditions and optimizes Schwann cell viability under oxidative stress conditions

Schwann cell proliferation capability is critical in peripheral

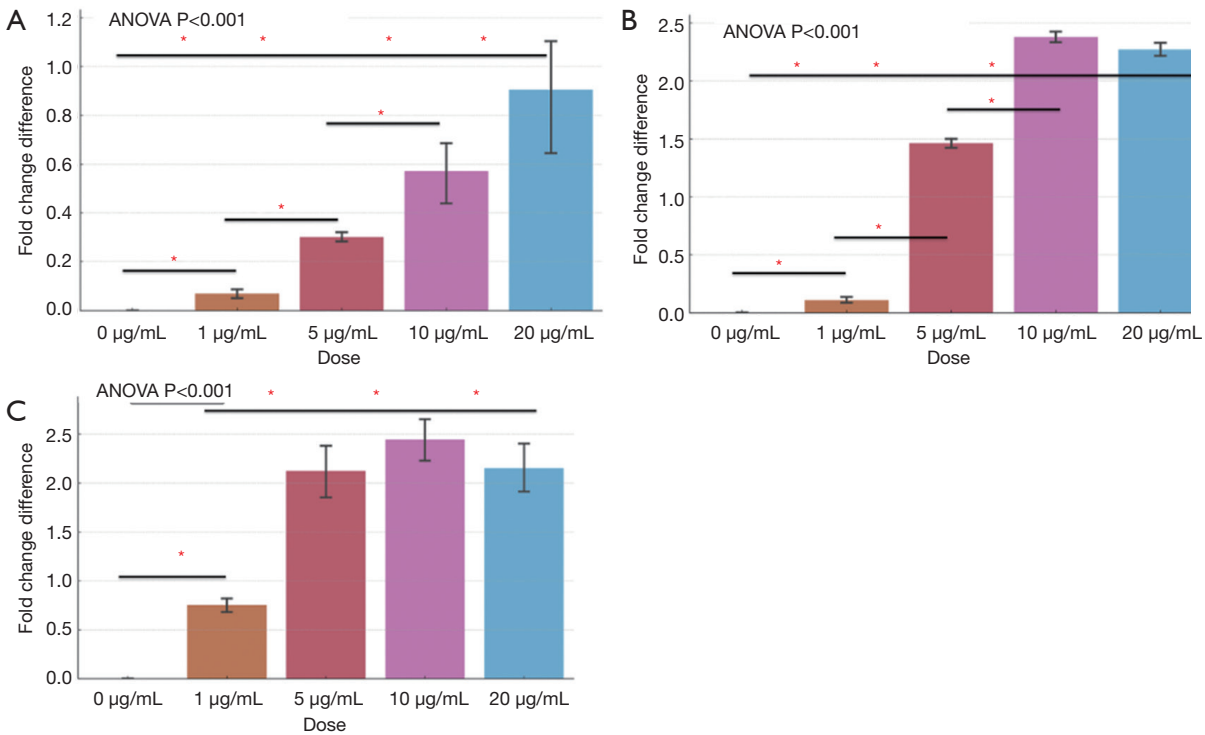

Figure 2 CCK-8 assay demonstrating Schwann cell proliferation. Each cell culture was treated with varying AFS-CM doses. The graphs represent the relative OD reading compared to cell culture pre-treated with 0 µg/mL of AFS-CM. A total of seven experiments were conducted. Graphs are as follows: fold change difference in Schwan cell viability at (A) 1 day (P<0.001); (B) 3 days (P<0.001); and (C) 5 days (P<0.001). Error bars signify a 95% confidence interval. ANOVA test assessed mean group differences. A *post-hoc* Tukey's HSD was performed to assess multiple comparisons of mean differences between groups. A "*" indicates a *post-hoc* Tukey HSD P value of <0.05. CCK-8, Cell Counting Kit-8; AFS-CM, amniotic fluid stem cell conditioned medium; OD, optical density; ANOVA, analysis of variance; HSD, honestly significant difference.

nerve recovery after injury. We sought to explore the mitogenic effect of AFS-CM on primary rat Schwann cell culture using a CCK-8 analysis. CCK-8 analysis revealed that AFS-CM caused a nearly dose-dependent increase in Schwann cell proliferation (*Figure 2*), indicating a mitogenic effect on primary rat Schwann cells. Our findings demonstrate that the optimal proliferative response to AFS-CM in cell culture was achieved at 10 µg/mL on both days 3 and 5. Additionally, the data indicate increased variability in the proliferative effects as the dosage of AFS-CM increased, suggesting a dose-dependent ceiling to its therapeutic efficacy.

Peripheral nerve Schwann cells must resist an inflammatory mediate oxidative burst that occurs soon after peripheral nerve injury to facilitate nerve recovery. We discovered that AFS-CM minimized the harmful effect of H_2O_2-mediated oxidative stress on primary Schwann cells. Our CCK-analysis revealed an AFS-CM mediated increase in fold change difference in Schwann cells in an oxidative stressed environment at the 24- and 48-hour period (*Figure 3*).

AFS-CM reduces cellular ROS via upregulation of catalase and SOD enzymes

ROS can serve as critical secondary messengers in normal cellular processes; however, its dysregulation secondary to external stressors can lead to cell damage and dysfunction. Accordingly, we sought to explore the effect of AFS-CM on cellular ROS when cells were exposed to increasing concentrations of H_2O_2. Cellular ROS levels were obtained for our primary rat Schwann cell culture after a 15-minute challenge of varying concentrations of H_2O_2. Our initial experiment revealed that H_2O_2 elicited a dose-dependent increase in cellular ROS from primary Schwann cells

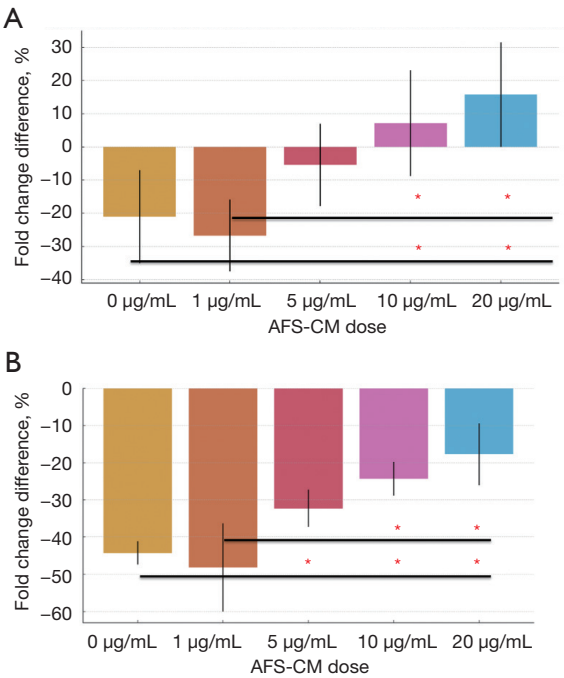

Figure 3 Fold change difference in Schwann cell proliferation after oxidative stress challenge with 80 µM of H_2O_2 for 1 hour. Cell cultures were treated with varying doses of AFS-CM (0, 1, 5, 10, 20 µg/mL) for 12 hours before the oxidative stress challenge. A positive control ("media only") denotes cell culture in which cells did not undergo oxidative stress challenge. The graphs represent the relative OD reading compared to positive control in which cells did not undergo oxidative stress. Graphs are as follows: (A) change difference at 24 hours (P<0.001); (B) change difference at 48 hours (P<0.001). Error bars denote a 95% confidence interval. ANOVA test assessed mean group differences. A *post-hoc* Tukey's HSD was performed to assess multiple comparisons of mean differences between groups. A "*" indicates a *post-hoc* Tukey HSD P value of <0.05. AFS-CM, amniotic fluid stem cell conditioned medium; OD, optical density; ANOVA, analysis of variance; HSD, honestly significant difference.

(*Figure 4A*). AFS-CM decreased cellular ROS levels when cells were challenged with 0 µM, 100 µM, 1 mM, and 4 mM of H_2O_2. Cells treated with AFS-CM exhibited statistically significant differences in ROS at varying concentrations of H_2O_2 (*Figure 4B*) with an increased concentration of AFS-CM. Interestingly, AFS-CM's attenuating effect on ROS generation was only observed at higher concentrations (4 mM) of H_2O_2. There was an increase in cell ROS generation with Schwann cells challenged with 0 µM of H_2O_2 pre-treated with an AFS-CM dose of 5 µg/mL and higher.

We sought to explore the effect of AFS-CM on facilitating cellular redox homeostasis in two key enzymes: catalase and SOD. These enzymes are critical for the Schwann cell after injury by mitigating oxidative stress and improving function, viability, and nerve recovery. SOD functions to convert superoxide free radicals to H_2O_2, whereas catalase converts H_2O_2 to H_2O and oxygen (O_2). Further experimentation revealed increased catalase and SOD activity with the administration of AFS-CM. Our analysis revealed increased catalase activity (as denoted by a decreased OD score) for cell cultures treated with 5 µg/mL of AFS-CM or more (*Figure 5A*). Schwann cell SOD activity was significantly increased with AFS-CM doses of 10 and 20 µg/mL (*Figure 5B*).

AFS-CM prevents stress-induced senescence in primary rat Schwann cells

Schwann cells run a risk of transforming into their stress-induced senescence phenotype after prolonged oxidative stress. This phenomenon is increasingly recognized as a key player in incomplete peripheral nerve recovery after injury (35). We found that AFS-CM developed a protective effect against stress-induced senescence in primary rat Schwann cells when challenged with H_2O_2. Our results reveal a lower proportion of senescent positive cells for cultures treated with 5, 10 and 20 µg/mL of AFS-CM when compared to 0 µg/mL of AFS-CM (*Figure 6*).

Discussion

Peripheral nerve injury confers significant morbidity for the afflicted, wherein most patients will be unable to attain pre-injury function (36,37). The Schwann cell is a critical component of peripheral nerve regeneration as it is vital in all parts of the regenerative process (38). Despite the innate regenerative capacity of peripheral nerves, ischemia, and the inflammatory process to clear out the debris from damage that occurs soon after peripheral nerve injury can lead to an unfavorable oxidative stressed environment that is cytotoxic to Schwann cells and hinder nerve regeneration. In this study, we found that AFS-CM has therapeutic effects to facilitate rat Schwann cell proliferation and survival under normative and oxidative stress conditions, reduce ROS production, and prevent cellular senescence under oxidative stress *in vitro*.

Our study revealed a near dose-dependent increase in cell

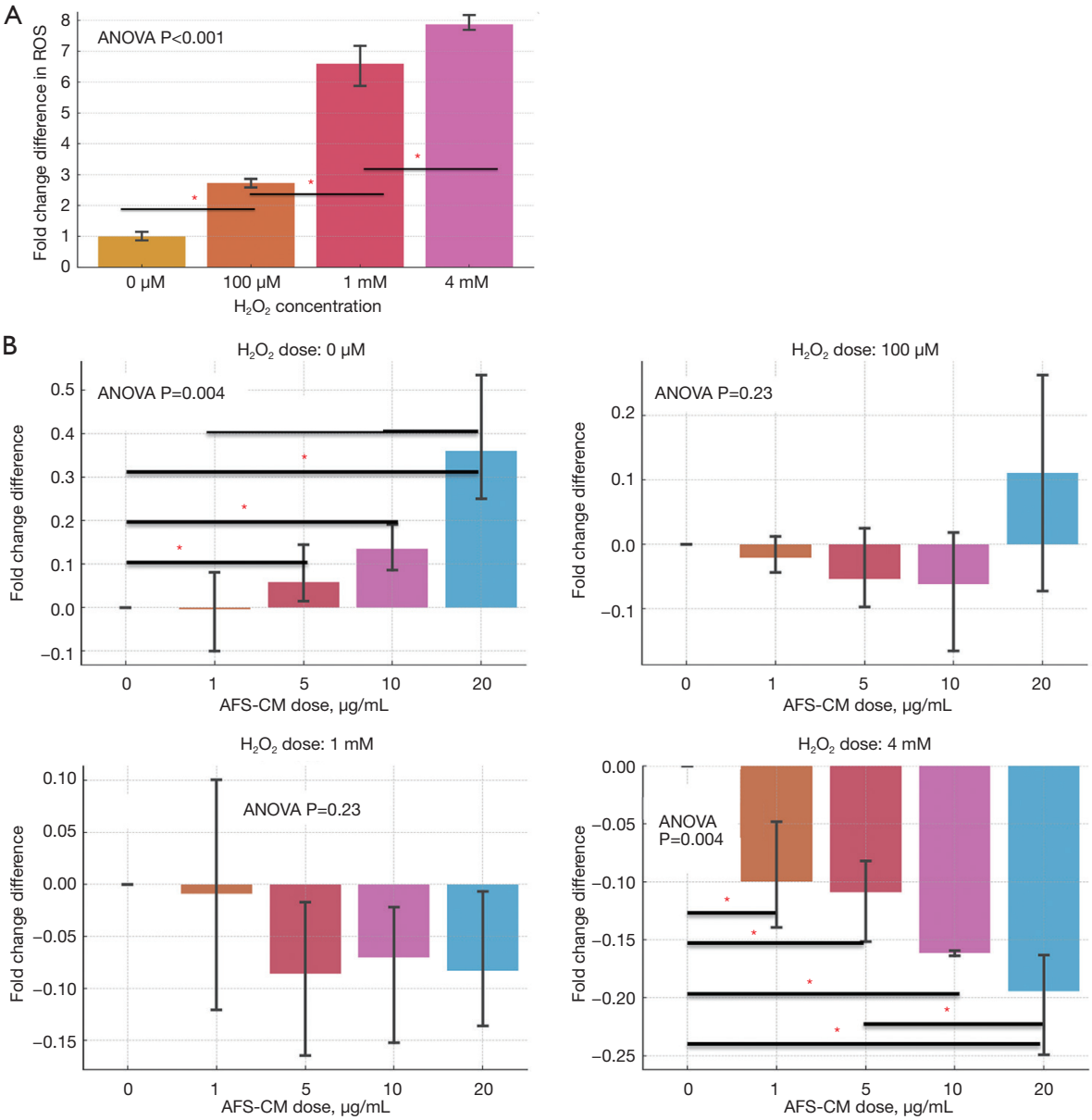

Figure 4 The following illustration represents the relative production of cellular ROS for primary Schwann cells pre-treated with varying concentrations of AFS-CM. The X-axis denotes the concentration of H_2O_2 for the oxidative stress challenge. (A) The positive control, which indicates an H_2O_2-related increase in cellular ROS species generation. (B) The fold change difference in cell reactive oxygen species generation compared to control (0 μg/mL of AFS-CM) at 100 μM, 1 mM, and 4 mM of H_2O_2. ANOVA test assessed mean group differences was performed. Error bars denote a 95% confidence interval. A *post-hoc* Tukey's HSD was performed to assess multiple comparisons of mean differences between groups. A "*" indicates a *post-hoc* Tukey HSD P value of <0.05. ROS, reactive oxygen species; AFS-CM, amniotic fluid stem cell conditioned medium; ANOVA, analysis of variance; HSD, honestly significant difference.

proliferation with increasing doses of AFS-CM. However, the cyto-proliferative effect of stem cell conditioned medium on Schwann cells is not unique to our study. Guo *et al.* (39) assessed the paracrine effects of human umbilical cord mesenchymal stem cells on primary rat Schwann cells. The authors reported an increase in Schwann cell viability at 24- and 48-hour time points when compared to control (P<0.01) and an increased rate of Schwann cell proliferation

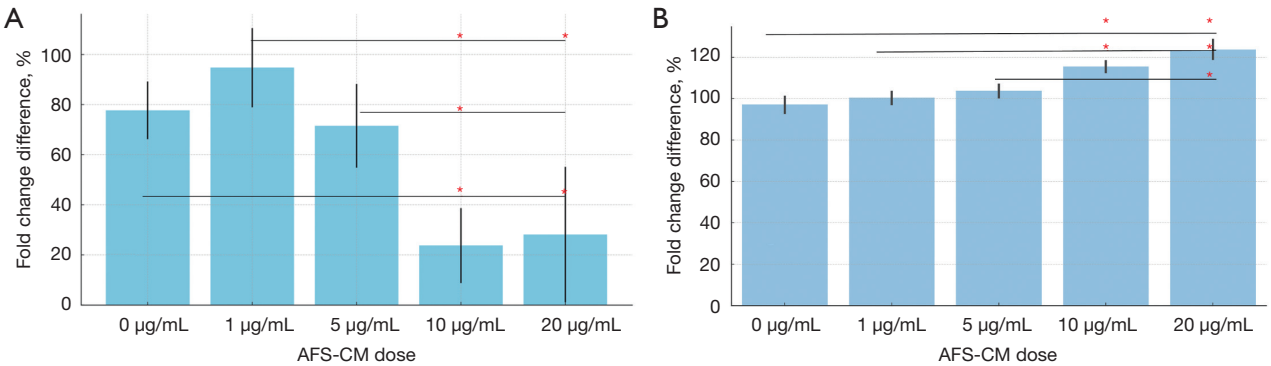

Figure 5 The following experiment results demonstrate the role of conditioned media on catalase and superoxide dismutase activity of primary rat Schwann cells. Here, non-converted H_2O_2 interacts with a proprietary probe, releasing a signal that can be measured colorimetrically. Catalase activity is inversely proportional to the OD signal. Superoxide dismutase activity is measured by SOD inhibition of xanthine oxidase according to the manufacturer's instructions. We report the fold change difference (in percent) of the OD signaling for Schwann cell cultures treated with varying concentrations of AFS-CM compared to control (medium only without H_2O_2). (A) The percent fold change difference in catalase activity when treated with varying concentrations of AFS-CM (P value <0.001) compared to the control. (B) The percent fold change difference in superoxide dismutase activity when treated with varying concentrations of AFS-CM (P value <0.001) compared to the control. Error bars represent a 95% confidence interval. Asterisk "*" denotes Tukey's HSD P value <0.05. OD, optical density; SOD, superoxide dismutase; AFS-CM, amniotic fluid stem cell conditioned medium; HSD, honestly significant difference.

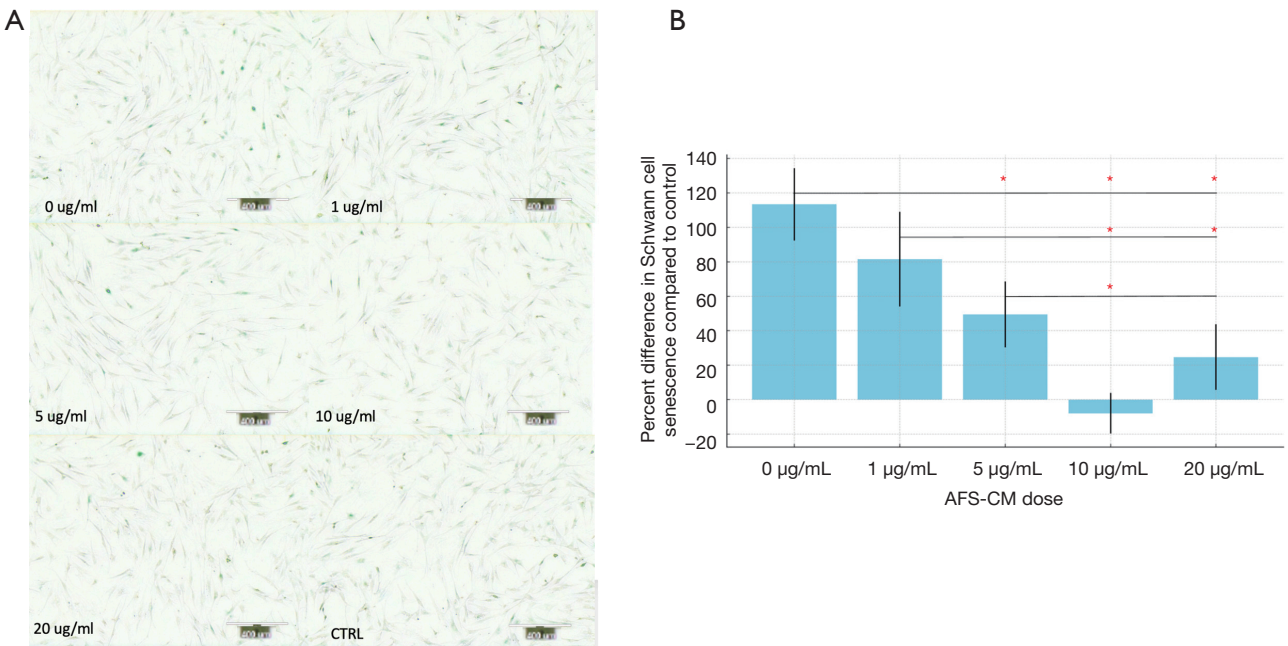

Figure 6 The following experiment results highlight the protective effect of AFS-CM against H_2O_2-mediated Schwann cell senescence. Briefly, Schwann cell culture was treated with varying doses of AFS-CM (0, 1, 5, 10, 20 µg/mL) and initially treated with 20 µM of H_2O_2 for 15 min followed by 10 µM of H_2O_2 for 15 min every 24 hours. Error bars represent 95% confidence intervals. (A) Schwann cell staining with S-beta galactosidase and senesced cells staining blue green. (B) Data are presented as the percent difference of cells staining positive for S-beta galactosidase compared to control (no H_2O_2 challenge). ANOVA test assessed mean group differences was performed (P<0.001). A *post-hoc* Tukey's HSD was performed. Asterisk (*) represents a P<0.05. Image scale bars =400 µm. "CTRL" denotes the control group. AFS-CM, amniotic fluid stem cell conditioned medium; ANOVA, analysis of variance; HSD, honestly significant difference.

at 48 hours ($P<0.01$). Similarly, we observed increased cell viability and proliferation at one, three, and five-day time points with increasing concentrations of AFS-CM. Of note, our results suggested an optimal proliferative effect of AFS-CM at 10 µg/mL at days 3 and 5, with higher doses conferring no additional benefit suggesting a ceiling effect with increment of dosages.

Interestingly, our findings reveal that AFS-CM had a protective effect against H_2O_2-induced oxidative stress at the 24- and 48-hour period. This may be due to the upregulation of cellular catalase and superoxide enzymes during the treatment of Schwann cell culture with AFS-CM. Free O_2^- radicals are produced during cellular respiration by the mitochondria and nitric oxide enzymes during both homeostasis and periods of intense inflammation (40). Catalase and SOD are antioxidants critical for the cellular defense against oxidative stress. SOD catalyzes the cell's dismutation of free O_2 radicals to molecular O_2 and H_2O_2 (41). Catalase in turn breaks down H_2O_2 to form O_2 and H_2O. The increased activity of these antioxidants noted in our experiments may be mediated by activation of the Nrf2/KEAP/ARE pathway as suggested by other investigators. Yan *et al.* (42) discovered that human placental mesenchymal stem cell conditioned medium protected against H_2O_2-induced oxidative damage and cellular apoptosis of fetal alveolar epithelial cells via the activation of Nrf2/KEAP1/ARE signaling pathway. This upregulation in antioxidants may cause a reduction in cellular ROS, thus ameliorating the excessive ROS-induced cellular damage. Interestingly, in our experiment, the protective effect of AFS-CM on reducing cellular ROS was more prominent when Schwann cells were exposed to higher levels of H_2O_2 (4 mM), suggesting that AFS-CM may only trigger the signaling cascades to restore the cellular homeostasis when the damage is beyond the cells' self-repair under oxidative stress. It is important to note that we saw an increase in cellular ROS when exposed to AFS-CM doses of 5 µg/mL in cells not challenged with H_2O_2. We speculate this to be due to an increased cell activity secondary to AFS-CM mitogenic effect on Schwann cells, as evidenced in *Figure 2*. To our knowledge, no previous studies have attempted to quantify the oxidative stress during peripheral nerve injury *in vivo*. Future research looking to explore the therapeutic potential of AFS-CM on peripheral nerve injury and regeneration should consider this magnitude of oxidative stress as this may play a role in the therapeutic efficacy of AFS-CM.

Still, it is important to note the AFS-CM's role in mitigating oxidative stress-induced senescence in our study. There is increasing evidence that Schwann cell senescence may be a culprit in failed and/or suboptimal peripheral nerve regeneration (17,43). Our findings reveal that AFS-CM mitigated the effects of repeated sublethal administration of H_2O_2 toward Schwann cells. ROS burst is an expected physiologic response soon after peripheral nerve injury (44,45) and can harm peripheral nerve regeneration. Büttner *et al.* (46) revealed that injury-induced inflammatory response was dramatically upregulated, resulting in a persistent hyper-inflammatory state up to 8 weeks after peripheral nerve injury. Several studies reveal that the neuroprotective effects of stem cells conditioned medium against oxidative stress via the upregulation of cellular antioxidants. Liu *et al.* (47) reported ROS-savaging activities of human-derived adipose mesenchymal stem cells on H_2O_2 treated rat Schwann cells. The authors highlight several studies demonstrating the role of exosomes in combating oxidative stress via the adaptive regulation of the nuclear factor erythroid 2-related factor (Nrf-2) defense system (48-50). Activation of the Nrf-2 defense system plays a role in preventing cellular stress-induced senescence. Shin *et al.* (51) demonstrated the role of Nrf-2 in preventing stress-induced senescence among H_2O_2-exposed human mesenchymal stem cells. The authors demonstrated a lower rate of stress-induced senescence with activation of Nrf2, a finding that was not seen among Nrf-2 knock-out mesenchymal stem cells. Thus, it can be suggested that the early activation of the Nrf2/KEAP1/ARE pathway may prevent stress-induced senescence of Schwann cells after peripheral nerve injury. Further experiments are warranted to investigate whether the effects of AFS-CM on cellular senescence were exerted through the activation of the Nrf-2 pathway.

Our study has limitations. We analyzed the therapeutic effect of AFS-CM *in vitro* only. It's important to note the intricate nature of multiple systems involved in peripheral nerve injuries *in vivo*, which may contribute to the therapeutic effect of AFS-CM. For example, Schwann cells' innate regenerative potential may vary based on host age, glucose metabolism (52), and baseline microenvironment before peripheral nerve injury. Additionally, our study assesses one-time AFS-CM delivery after oxidative stress challenge on rat Schwann cells. The optimal timing for treatment following injury needs further exploration as it may be a key factor in understanding the translational therapeutic capability of AFS-CM to *in-vivo* models. Nonetheless, our study demonstrates the proliferative effect

of AFS-CM on Schwann cells without affecting the cell viability over time. AFS-CM also demonstrates its ability to improve Schwann cell survival under oxidative stress via the upregulation of cellular antioxidants and inhibition of cell senescence. Our lab is currently investigating the *in vivo* therapeutic effect of AFS-CM on peripheral nerve regeneration after transection injury.

Conclusions

In conclusion, this study demonstrates the therapeutic potential of AFS-CM in promoting Schwann cell proliferation and enhancing cellular resilience against oxidative stress in peripheral nerve injuries. The observed protective effects, particularly the upregulation of antioxidant enzymes, suggest that AFS-CM may facilitate peripheral nerve recovery after injury.

Acknowledgments

None.

Footnote

Reporting Checklist: The authors have completed the ARRIVE reporting checklist. Available at https://atm.amegroups.com/article/view/10.21037/atm-24-107/rc

Data Sharing Statement: Available at https://atm.amegroups.com/article/view/10.21037/atm-24-107/dss

Peer Review File: Available at https://atm.amegroups.com/article/view/10.21037/atm-24-107/prf

Funding: None.

Conflicts of Interest: All authors have completed the ICMJE uniform disclosure form (available at https://atm.amegroups.com/article/view/10.21037/atm-24-107/coif). The authors have no conflicts of interest to declare.

Ethical Statement: The authors are accountable for all aspects of the work in ensuring that questions related to the accuracy or integrity of any part of the work are appropriately investigated and resolved. The experiments of the present study were approved by the Institution of Animal Care and Use Committee (IACUC) at Atrium Wake Forest Baptist Health (IACUC # A19-101), in compliance with institutional guidelines for the care and use of animals.

References

1. Xu G, Zou X, Dong Y, et al. Advancements in autologous peripheral nerve transplantation care: a review of strategies and practices to facilitate recovery. Front Neurol 2024;15:1330224.
2. Dong Y, Lu H. Editorial: Surgical treatment of peripheral neuropathic pain, peripheral nerve tumors, and peripheral nerve injury. Front Neurol 2023;14:1266638.
3. Dong Y, Alhaskawi A, Zhou H, et al. Imaging diagnosis in peripheral nerve injury. Front Neurol 2023;14:1250808.
4. Beris A, Gkiatas I, Gelalis I, et al. Current concepts in peripheral nerve surgery. Eur J Orthop Surg Traumatol 2019;29:263-9.
5. Li R, Liu Z, Pan Y, et al. Peripheral nerve injuries treatment: a systematic review. Cell Biochem Biophys 2014;68:449-54.
6. Grinsell D, Keating CP. Peripheral nerve reconstruction after injury: a review of clinical and experimental therapies. Biomed Res Int 2014;2014:698256.
7. Faroni A, Mobasseri SA, Kingham PJ, et al. Peripheral nerve regeneration: experimental strategies and future perspectives. Adv Drug Deliv Rev 2015;82-83:160-7.
8. Gonzalez-Perez F, Udina E, Navarro X. Extracellular matrix components in peripheral nerve regeneration. Int Rev Neurobiol 2013;108:257-75.
9. Coleman MP, Freeman MR. Wallerian degeneration, wld(s), and nmnat. Annu Rev Neurosci 2010;33:245-67.
10. Gaudet AD, Popovich PG, Ramer MS. Wallerian degeneration: gaining perspective on inflammatory events after peripheral nerve injury. J Neuroinflammation 2011;8:110.
11. Jessen KR, Arthur-Farraj P. Repair Schwann cell update: Adaptive reprogramming, EMT, and stemness in regenerating nerves. Glia 2019;67:421-37.
12. Jessen KR, Mirsky R. The Success and Failure of the

Schwann Cell Response to Nerve Injury. Front Cell Neurosci 2019;13:33.
13. Jessen KR, Mirsky R. The repair Schwann cell and its function in regenerating nerves. J Physiol 2016;594:3521-31.
14. Qiu J, Yang X, Wang L, et al. Isoquercitrin promotes peripheral nerve regeneration through inhibiting oxidative stress following sciatic crush injury in mice. Ann Transl Med 2019;7:680.
15. Hoben GM, Ee X, Schellhardt L, et al. Increasing Nerve Autograft Length Increases Senescence and Reduces Regeneration. Plast Reconstr Surg 2018;142:952-61.
16. Saheb-Al-Zamani M, Yan Y, Farber SJ, et al. Limited regeneration in long acellular nerve allografts is associated with increased Schwann cell senescence. Exp Neurol 2013;247:165-77.
17. Poppler LH, Ee X, Schellhardt L, et al. Axonal Growth Arrests After an Increased Accumulation of Schwann Cells Expressing Senescence Markers and Stromal Cells in Acellular Nerve Allografts. Tissue Eng Part A 2016;22:949-61.
18. Wei C, Guo Y, Ci Z, et al. Advances of Schwann cells in peripheral nerve regeneration: From mechanism to cell therapy. Biomed Pharmacother 2024;175:116645.
19. Gwam C, Emara AK, Mohamed N, et al. Amniotic Stem Cell-Conditioned Media for the Treatment of Nerve and Muscle Pathology: A Systematic Review. Surg Technol Int 2021;38:407-14.
20. Gwam C, Ohanele C, Hamby J, et al. Human placental extract: a potential therapeutic in treating osteoarthritis. Ann Transl Med 2023;11:322.
21. Haastert K, Mauritz C, Chaturvedi S, et al. Human and rat adult Schwann cell cultures: fast and efficient enrichment and highly effective non-viral transfection protocol. Nat Protoc 2007;2:99-104.
22. Penicillin-Streptomycin (10,000 U/mL) [cited 2024 Aug 30]. Available online: https://www.thermofisher.com/order/catalog/product/15140122
23. Fetal Bovine Serum, Value, heat inactivated (formerly USDA-approved in North America or qualified, Brazil in other regions) [cited 2024 Aug 30]. Available online: https://www.thermofisher.com/order/catalog/product/A5256801?gclid=Cj0KCQjww5u2BhDeARIsALBuLnMWVwaBC6-oyhD6nJw_tA6X_ie3K7kzem4YNwS3tig09wsmR6drYdMaAjWqEALw_wcB&source=google_shopping&ISO_CODE=us&LANG_CODE=en&ef_idCj0KCQjww5u2BhDeARIsALBuLnMWVwaBC6-oyhD6nJw_tA6X_ie3K7kzem4YNwS3tig09wsmR6drYdMaAjWqEALw_wcB:G:s&ppc_id=PLA_BID_goog_PrivateLabel_20282129496_147241558061_A5256801__66293 7884120_61478710325324 6353&ev_chn=shop&cid=0se_gaw_14062023_ERY23A&ef_id=Cj0KCQjww5u2BhDeARIsALBuLnMWVwaBC6-oyhD6nJw_tA6X_ie3K7kzem4YNwS3tig09wsmR6drYdMaAjWqEALw_wcB:G:s&s_kwcid=AL!3652!3!662937884120!!!g!2089231252079!!20282129496!147241558061&source=google_shopping&ISO_CODE=us&LANG_CODE=en&gad_source=
24. MilliporeSigma Amicon Ultra-2 Centrifugal Filter Units: Filters and Filtration: Centrifugal | Fisher Scientific [cited 2024 Aug 30]. Available online: https://www.fishersci.com/shop/products/emd-millipore-amicon-ultra-15-centrifugal-filter-units-15/p-4902700
25. Bradford Dye Reagent, Ready-to-Use soln. [cited 2024 May 5]. Available online: https://www.thermofisher.com/order/catalog/product/J61522.K2?gclid=Cj0KCQjw_-GxBhC1ARIsADGgDjuLXfbLuIcyyCUutMJQrkZ3cNtWciN2hd0ZajC6B6-dp6yJ576r_d8aAvbbEALw_wcB&cid=lcd_dig_sbu_r02_us_cp1517_pjt8642_col019235_0se_gaw_dy_pur_&ef_id=Cj0KCQjw_-GxBhC1ARIsADGgDjuLXfbLuIcyyCUutMJQrkZ3cNtWciN2hd0ZajC6B6-dp6yJ576r_d8aAvbbEALw_wcB:G:s&s_kwcid=AL!3652!3!603983824448!!!g!!!15827394693!132093184476&gad_source=1
26. Ma X, Elsner E, Cai J, et al. Peripheral Nerve Regeneration with Acellular Nerve Allografts Seeded with Amniotic Fluid-Derived Stem Cells. Stem Cells Int 2022;2022:5240204.
27. Cell Counting Kit-8 (CCK-8) Cell Proliferation / Cytotoxicity Assay Dojindo [cited 2024 May 5]. Available online: https://www.dojindo.com/products/CK04/
28. 96-Well Cell Culture Plates | Thermo Fisher Scientific - US [cited 2024 Aug 30]. Available online: https://www.thermofisher.com/us/en/home/life-science/cell-culture/cell-culture-plastics/cell-culture-plates/96-well-cell-culture-plates.html
29. Results for "ab186027 ab186027" | Abcam: antibodies, proteins, kits... [cited 2024 May 5]. Available online: https://www.abcam.com/products?keywords=ab186027+%28ab186027%29&gad_source=1&gclid=Cj0KCQjw_-GxBhC1ARIsADGgDjv-DEhUzo5kDBKvgfKSSv1RjHXMfZ6Vz2OmVJBB8ILB1_UDb7Euh3kaAkVGEALw_wcB&gclsrc=aw.ds
30. Cellular ROS Assay Kit (Red) (ab186027) | Abcam [cited 2024 May 3]. Available online: https://www.abcam.com/products/assay-kits/cellular-ros-assay-kit-red-ab186027.html
31. Wang Z, Wei D, Xiao H. Methods of cellular senescence

induction using oxidative stress. Methods Mol Biol 2013;1048:135-44.
32. beta Galactosidase Staining Kit (ab102534) | Abcam [cited 2024 May 3]. Available online: https://www.abcam.com/products/assay-kits/beta-galactosidase-staining-kit-ab102534.html
33. Catalase Activity Assay Kit (Colorimetric/Fluorometric) (ab83464/K773-100)| Abcam [cited 2024 May 5]. Available online: https://www.abcam.com/products/assay-kits/catalase-activity-assay-kit-colorimetricfluorometric-ab83464.html
34. Superoxide Dismutase Activity Assay Kit (Colorimetric) (ab65354/K335-100) | Abcam [cited 2024 May 5]. Available online: https://www.abcam.com/products/assay-kits/superoxide-dismutase-activity-assay-kit-colorimetric-ab65354.html
35. Fuentes-Flores A, Geronimo-Olvera C, Girardi K, et al. Senescent Schwann cells induced by aging and chronic denervation impair axonal regeneration following peripheral nerve injury. EMBO Mol Med 2023;15:e17907.
36. Kuffler DP, Foy C. Restoration of Neurological Function Following Peripheral Nerve Trauma. Int J Mol Sci 2020;21:1808.
37. Hussain G, Wang J, Rasul A, et al. Current Status of Therapeutic Approaches against Peripheral Nerve Injuries: A Detailed Story from Injury to Recovery. Int J Biol Sci 2020;16:116-34.
38. Lu Y, Li R, Zhu J, et al. Fibroblast growth factor 21 facilitates peripheral nerve regeneration through suppressing oxidative damage and autophagic cell death. J Cell Mol Med 2019;23:497-511.
39. Guo ZY, Sun X, Xu XL, et al. Human umbilical cord mesenchymal stem cells promote peripheral nerve repair via paracrine mechanisms. Neural Regen Res 2015;10:651-8.
40. Stavely R, Nurgali K. The emerging antioxidant paradigm of mesenchymal stem cell therapy. Stem Cells Transl Med 2020;9:985-1006.
41. Superoxide Dismutase - an overview | ScienceDirect Topics [cited 2021 Jan 17]. Available online: https://www.sciencedirect.com/topics/neuroscience/superoxide-dismutase
42. Yan X, Fu X, Jia Y, et al. Nrf2/Keap1/ARE Signaling Mediated an Antioxidative Protection of Human Placental Mesenchymal Stem Cells of Fetal Origin in Alveolar Epithelial Cells. Oxid Med Cell Longev 2019;2019:2654910.
43. Yoshizawa H, Senda D, Natori Y, et al. End-to-Side Neurorrhaphy as Schwann Cells Provider to Acellular Nerve Allograft and Its Suitable Application. PLoS One 2016;11:e0167507.
44. Hervera A, De Virgiliis F, Palmisano I, et al. Reactive oxygen species regulate axonal regeneration through the release of exosomal NADPH oxidase 2 complexes into injured axons. Nat Cell Biol 2018;20:307-19.
45. Panthi S, Gautam K, Jung J. Correction to: Roles of nitric oxide and ethyl pyruvate after peripheral nerve injury. Inflamm Regen 2019;39:1.
46. Büttner R, Schulz A, Reuter M, et al. Inflammaging impairs peripheral nerve maintenance and regeneration. Aging Cell 2018;17:e12833.
47. Liu B, Kong Y, Shi W, et al. Exosomes derived from differentiated human ADMSC with the Schwann cell phenotype modulate peripheral nerve-related cellular functions. Bioact Mater 2022;14:61-75.
48. Bessa-Gonçalves M, Silva AM, Brás JP, et al. Fibrinogen and magnesium combination biomaterials modulate macrophage phenotype, NF-kB signaling and crosstalk with mesenchymal stem/stromal cells. Acta Biomater 2020;114:471-84.
49. Lv W, Deng B, Duan W, et al. Schwann Cell Plasticity is Regulated by a Weakened Intrinsic Antioxidant Defense System in Acute Peripheral Nerve Injury. Neuroscience 2018;382:1-13.
50. Balakrishnan A, Belfiore L, Chu TH, et al. Insights Into the Role and Potential of Schwann Cells for Peripheral Nerve Repair From Studies of Development and Injury. Front Mol Neurosci 2020;13:608442.
51. Shin JH, Jeon HJ, Park J, et al. Epigallocatechin-3-gallate prevents oxidative stress-induced cellular senescence in human mesenchymal stem cells via Nrf2. Int J Mol Med 2016;38:1075-82.
52. Rawat A, Morrison BM. Metabolic Transporters in the Peripheral Nerve-What, Where, and Why? Neurotherapeutics 2021;18:2185-99.

Cite this article as: Gwam C, Mohamed N, Ogunsola AS, Brown MG, Henry KA, Ma X. Amniotic fluid stem cell conditioned medium's role in Schwann cell proliferation, survival, and cellular antioxidant activity under normative and oxidative stress conditions. Ann Transl Med 2025;13(1):1. doi: 10.21037/atm-24-107